

**NIH PUBLIC ACCESS**

Author manuscript

*Chem Commun (Camb)*. Author manuscript; available in PMC 2016 October 21.

Published in final edited form as:

*Chem Commun (Camb)*. 2015 October 21; 51(82): 15192–15195. doi:10.1039/c5cc06099k.**Luminogenic iridium azide complexes****Jun Ohata<sup>a</sup>, Farrukh Vohidov<sup>a</sup>, Amirhossein Aliyan<sup>a</sup>, Kewei Huang<sup>a</sup>, Angel A. Martí<sup>a</sup>, and Zachary T. Ball<sup>a</sup>**

zb1@rice.edu; Tel: 1-713-348-6159

<sup>a</sup> Department of Chemistry, Rice University, Houston, Texas 77005, USA**Abstract**

The synthesis and characterization of luminogenic, bioorthogonal iridium probes is described. These probes exhibit long fluorescent lifetimes amenable to time-resolved applications. A simple, modular synthesis via 5-azidophenanthroline allows structural variation and allows optimization of cell labeling.

Luminogenic bioorthogonal probes have emerged as essential tools to visualize specific biomolecules in complex and confined environments, by virtue of “turn-on” emission and exquisite selectivity toward unique functional groups. Transition-metal complexes as labeling dyes have potential benefits such as red to near-IR emission, long photoluminescence lifetime, low photobleaching, stability in oxidative environments, and synthetic ease. Although they complement organic fluorogenic probes,<sup>2-5</sup> transition-metal luminogenic probes remain relatively little-studied. In this paper, we describe the first transition-metal complex-based luminogenic azide probe appropriate for biological imaging: an iridium emitter with red photoluminescence, long emission lifetimes, efficient “turn-on” photoluminescence, and cell penetration and labeling capabilities.

Much of the development of luminogenic transition-metal complexes has focused on sensor development,<sup>6-9</sup> while bioorthogonal probe development remains less studied.<sup>10</sup> Yet metal-based emitters have tunable emission and are prepared by simple synthesis. Furthermore, transition-metal complexes can have superior performance in two-photon imaging.<sup>11,12</sup> Octahedral metal complexes are 3D objects, less prone to aggregation, membrane association, and DNA interactions common with planar organic fluorophores. Indeed, appending polyarene units to octahedral complexes is a common method to induce DNA interactions in otherwise inert complexes.<sup>13,14</sup> Perhaps most significantly, the intrinsic triplet excited-state of transition-metal complexes results in long photoluminescence lifetime (10 ns to 100 μs or longer). Together with “time-gated” detection methods, photoluminescent probes would allow independent analysis of multiple dyes with similar emission profiles and/or images with significantly lower background noise. Recently, a study described turn-on imaging with rhenium compounds by means of [4 + 2] cycloaddition reaction.<sup>15</sup> A recent

Correspondence to: Zachary T. Ball.

Electronic Supplementary Information (ESI) available: experimental procedures complete characterization data, and supplemental luminescence figures. See DOI: 10.1039/x0xx00000x

report of DNA staining with dinuclear ruthenium complexes confirms the potential of time-resolved imaging.<sup>16</sup> Likewise, pH-responsive iridium complexes are effective for time-resolved imaging of the cytoplasm.<sup>17</sup>

Our probe design was guided by our work<sup>7</sup> indicating that the photoluminescence quantum efficiency of an octahedral phenanthroline–iridium complex is affected by substituents at the phenanthroline 5-position, which seem capable of modulating the contribution of non-radiative pathways to the relaxation of a metal-to-ligand charge transfer (MLCT) excited state.<sup>19</sup> Similar octahedral iridium complexes are well-suited to cellular and sub-cellular imaging.<sup>20-23</sup> We hypothesized that an azide might serve as a similarly non-radiative quencher for Ir(ppy)<sub>2</sub>(phen) (ppy = 2-phenylpyridine and phen = 1,10-phenanthroline). Although the efficacy of azide-based quenching can be unpredictable even in relatively well-studied organic fluorophores,<sup>24</sup> we designed azide-substituted complexes **5**. Three azide complexes **5a-5c** were isolated (78-93%) by reaction of amine precursors **4** with *t*-butyl nitrite and trimethylsilyl azide<sup>25</sup> after precipitation from ether (Fig. 1a).

A more convergent and efficient preparation of the desired complexes (**5**) was also developed from 5-azidophenanthroline (**3**), prepared for the first time here by epoxide ring-opening and subsequent elimination<sup>1</sup> of an epoxide precursor **1** (all attempts at diazotization of 5-aminophenanthroline were unsuccessful). In this way, 5-azidophenanthroline (**3**) was purified in high yield, and complexation with [Ir(ppy)<sub>2</sub>(MeCN)<sub>2</sub>][PF<sub>6</sub>] afforded **5a** (74%). The preparation of complex **5** from azidophenanthroline **3** is a more convergent route that facilitates variation on the 2-phenylpyridine ligand. With an eye toward investigating the effects of different substituents, we synthesized complexes **5b**, **5c**, **5d**, incorporating water-solubilizing and anionic groups.

Consistent with photoluminescence “turn-on” behavior, the azide complexes show very weak photoluminescence, while the triazole products (**6**) of a cycloaddition reaction with phenylacetylene show bright emission. Fig. 1b shows the emission spectra of the carboxyazide complex **5b** (red line) and the carboxytriazole complex **6b** (blue line). The photophysical properties of these complexes are summarized in Table 1. Both parent and carboxylate-functionalized complexes show significant enhanced photoluminescence upon the triazole ring formation (13× for **6a**, 19× for **6b**, relative to the azide complexes). Gratifyingly, the amine complexes **4a** and **4b** also show minimal luminescence. As expected, the triazole complex **6a** has significant emission in the region of relative tissue transparency above 650 nm (emission maximum: 637 nm).<sup>27,28</sup> Photoluminescence lifetimes of the triazole complexes (~60 ns) are significantly longer than that of typical organic fluorophores (<5 ns). The triazole **6b** exhibited useful quantum efficiency in aqueous solution (4.5%), in contrast to lower efficiencies often observed with transition-metal emitters due to a large non-radiative rate constant. Moreover, the lifetime and brightness are greatly increased in a non-solution application; the lifetime of a carboxytriazole complex immobilized on PVDF membrane (vide infra) is ~1 μs, rendering these complexes useful for surface imaging.

The kinetics of azide-alkyne cycloadditions were straightforward and consistent with an electron-deficient azide. We first tested copper-catalyzed reactions with a triazole ligand using a microplate reader (Fig. 2a).<sup>26</sup> Complete “turn-on” of the photoluminescence was

observed within 20 min (Fig. 2a, red rectangles), while no reaction occurred in the absence of copper catalyst (blue triangles). Similar trends were observed for the other azide complexes **5a-5c** (ESI). A recent report suggests that the kinetics of metal-free cycloaddition reactions are governed by electronics matching of the two reactants to favor normal-demand or inverse-demand cycloaddition pathways.<sup>29</sup> To further investigate reactivity of the azido Ir complex, we monitored the photoluminescence enhancement of reaction of **5d** with an electron-rich cycloalkyne (BCN, **8a**) and electron-poor dibenzocyclooctyne (DBCO, **9**) (Fig. 2b, c). Although both of reactions shows increase of photoluminescence, the reaction of **5d** with **8a** proceeded considerably faster than **9**; Assuming a pseudo-first-order reaction, the apparent half-life of the reaction of **8a** was much shorter than that of **9** (19 min vs 200 min). These results identify possible optimal alkyne partners for labeling applications, and imply that the complexes act as electron-deficient azides in cycloaddition reactions.

Having confirmed the luminogenic properties of the iridium complexes, we examined their suitability for protein labeling. Alkyne-tagged BSA<sup>30</sup> was treated with the iridium-azide complex **5b** in the presence of CuSO<sub>4</sub>, sodium ascorbate, and THPTA. After SDS-PAGE and membrane transfer, a strong photoluminescence band was observed only in the presence of a copper (II) salt and alkyne tag, consistent with selective tagging (Fig. 3b).

The long photoluminescence lifetime of the Ir complexes could be used to discriminate among emissive dyes and remove background emission.<sup>31</sup> We analyzed mixtures of two dye-labeled proteins, the BSA-Ir conjugate and maltose binding protein labeled with rhodamine (MBP-TAMRA), which has an emission profile similar to BSA-Ir. A gel blot analysis of the mixture revealed two photoluminescent bands with similar steady-state intensities (Fig. 3c and ESI). However, the emission lifetimes were markedly different (~1  $\mu$ s vs <100 ns, Fig. 4a). Following concepts we outlined previously,<sup>31</sup> a 1000–1500-ns time window was chosen to minimize background MBP-TAMRA. Fig. 4b compares the emission intensity of the proteins under steady-state (left) and time-resolved (right) analysis. Time-gating and the unique photophysical properties of the iridium complex allow a 20-fold diminution in signal from the model background TAMRA signal. Interestingly, time-gating methods also eliminated a significant background emission from the PVDF membrane (ESI).

Finally, luminogenic iridium azides proved capable cellular imaging agents. U2OS cells were pre-treated with reactive alkyne **8b**, washed, and fixed. Attempted imaging with complex **5a** was disappointing, as photoluminescence was observed in negative controls (Fig. 5a). Accumulation and membrane association of hydrophobic, cationic dyes is well known, and thus we had incorporated carboxylate or sulfate groups (**5b** and **5d**) to alter the charge. The anionic sulfate complex **5d** succeeded in minimizing background staining (Fig. 5a). The observation of background non-covalent staining with **5a** and **5b** could be due to background photoluminescence of either the unreacted azide or (more probably) the reduced aniline compound, possibly amplified by solvchromatic behavior of hydrophilic dyes.<sup>30,32,33</sup> Through chemical manipulation of the physical properties of the azide complexes, we successfully imaged alkyne-modified biopolymers while preventing background photoluminescence.

Two-photon excitation is a powerful imaging tool, and iridium complex **5d** exhibited robust two-photon imaging. Motivated in part by the large two-photon cross-section of similar octahedral metal complexes,<sup>34</sup> we irradiated alkyne-modified cells with a 860-nm laser and saw clean cell images with minimal background in the absence of alkyne (Fig. 5b). Similar to results from one-photon excitation, the best images with minimal background were obtained with anionic complex **5d**. Gratifyingly and consistent with the primary motivation for two-photon excitation in general, our initial studies indicate improved signal-to-noise with 860-nm excitation.

In summary, the facile synthesis of luminogenic azido iridium complexes enables their use for biomolecule labeling and imaging. These iridium complexes have large Stokes shifts, exhibit photoluminescence “turn-on” behaviour upon triazole formation, have long photoluminescence lifetimes, and are amenable to two-photon imaging. The use of time-gating removes unwanted signal from spurious emitters. The simple, modular synthesis allowed access to an anionic derivative that prevents background emission. Since phenanthroline is a common ligand motif for photoactive transition-metal complexes (e.g. Ru,<sup>35</sup> Re,<sup>36</sup> Pt<sup>37</sup>), the facile synthesis of 5-azidophenanthroline described here could help expand the portfolio of functionalized photoactive complexes.

## Supplementary Material

Refer to Web version on PubMed Central for supplementary material.

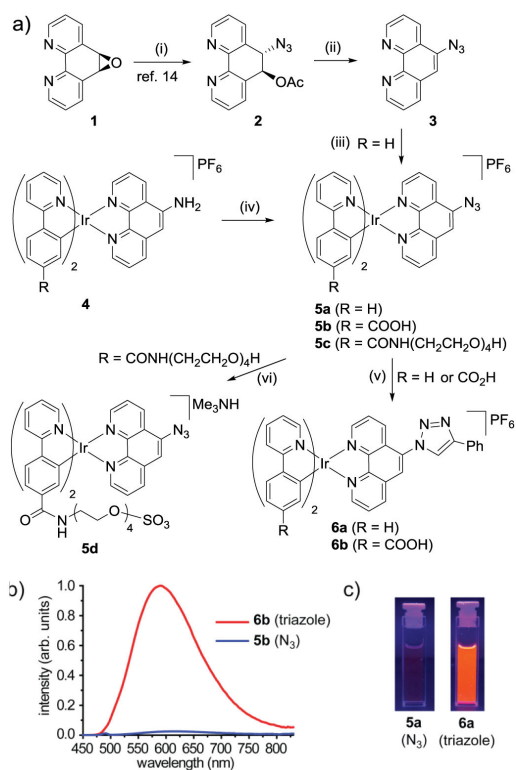
## Acknowledgments

We acknowledge support from the National Institutes of Health under grant number 5R21CA170625, from the Robert A. Welch Foundation Research Grants C-1680 and C-1743, and from the National Science Foundation (CHE-1055569).

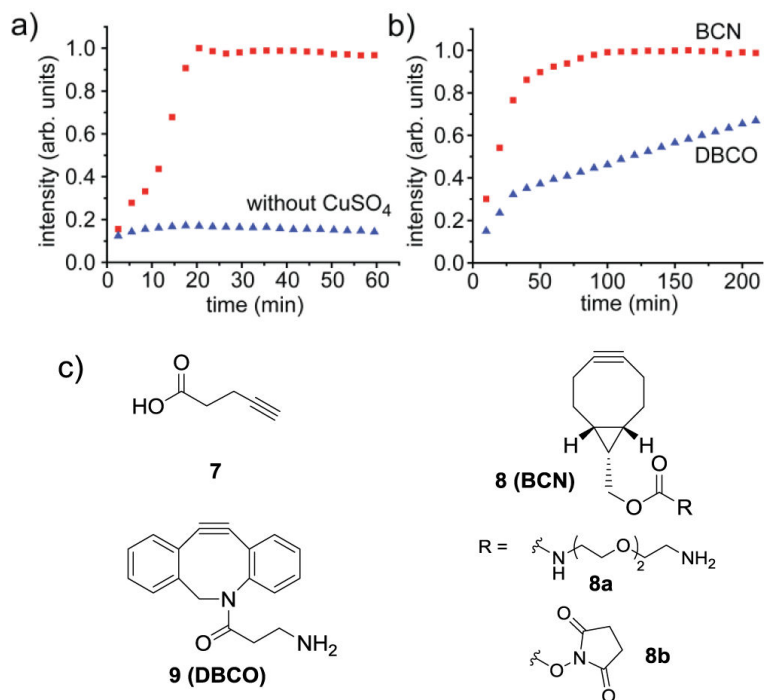
## References

1. Sanfilippo C, Nicolosi G. *Tetrahedron: Asymmetry*. 2008; 19:2171.
2. Hsu TL, Hanson SR, Kishikawa K, Wang SK, Sawa M, Wong CH. *Proc. Natl. Acad. Sci. U. S. A.* 2007; 104:2614. [PubMed: 17296930]
3. Le Droumaguet C, Wang C, Wang Q. *Chem. Soc. Rev.* 2010; 39:1233. [PubMed: 20309483]
4. Friscourt F, Fahrni CJ, Boons GJ. *J. Am. Chem. Soc.* 2012; 134:18809. [PubMed: 23095037]
5. Shieh P, Siegrist MS, Cullen AJ, Bertozzi CR. *Proc. Natl. Acad. Sci. U. S. A.* 2014; 111:5456. [PubMed: 24706769]
6. Zhang R, Ye ZQ, Wang GL, Zhang WZ, Yuan JL. *Chem. Eur. J.* 2010; 16:6884. [PubMed: 20458707]
7. Huang KW, Bulik IW, Marti AA. *Chem. Commun.* 2012; 48:11760.
8. Shiu H-Y, Wong M-K, Che C-M. *Chem. Commun.* 2011; 47:4367.
9. Saneyoshi H, Ito Y, Abe H. *J. Am. Chem. Soc.* 2013; 135:13632. [PubMed: 24010717]
10. Lo KK-W, Chan BT-N, Liu H-W, Zhang KY, Li SP-Y, Tang TS-M. *Chem. Commun.* 2013; 49:4271.
11. Botchway SW, Charnley M, Haycock JW, Parker AW, Rochester DL, Weinstein JA, Williams JAG. *Proc. Natl. Acad. Sci. U. S. A.* 2008; 105:16071. [PubMed: 18852476]
12. Hanczyc P, Norden B, Samoc M. *Dalton Trans.* 2012; 41:3123. [PubMed: 22293935]
13. Aguirre JD, Angeles-Boza AM, Chouai A, Pellois JP, Turro C, Dunbar KR. *J. Am. Chem. Soc.* 2009; 131:11353. [PubMed: 19624128]

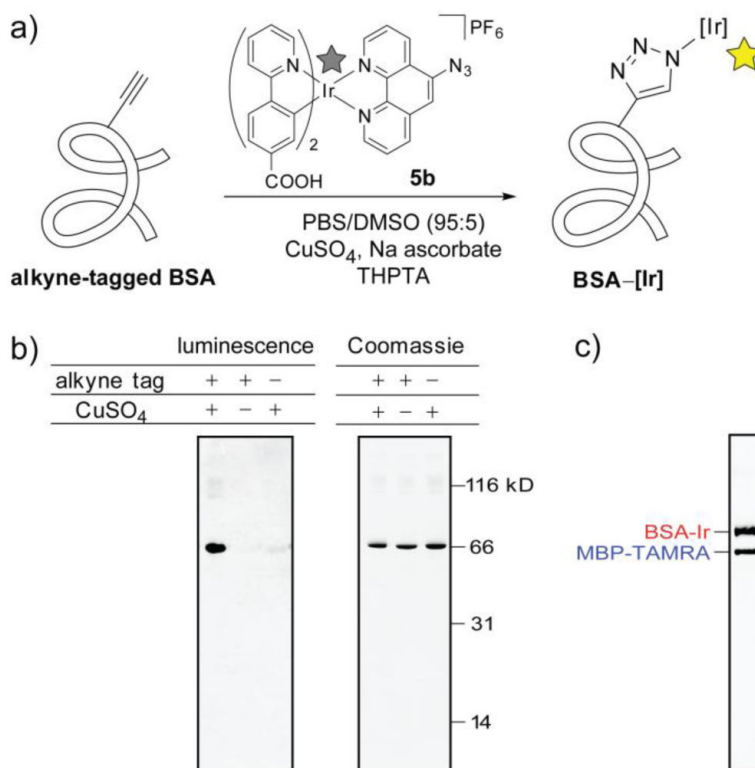
14. Komor AC, Barton JK. *Chem. Commun.* 2013; 49:3617.
15. Choi AW-T, Tso KK-S, Yim VM-W, Liu H-W, Lo KK-W. *Chem. Commun.* 2015; 51:3442.
16. Baggaley E, Gill MR, Green NH, Turton D, Sazanovich IV, Botchway SW, Smythe C, Haycock JW, Weinstein JA, Thomas JA. *Angew. Chem. Int. Ed.* 2014; 53:3367.
17. Murphy L, Congreve A, Palsson LO, Williams JAG. *Chem. Commun.* 2010; 46:8743.
18. Suzuki K, Kobayashi A, Kaneko S, Takehira K, Yoshihara T, Ishida H, Shiina Y, Oishic S, Tobita S. *Phys. Chem. Chem. Phys.* 2009; 11:9850. [PubMed: 19851565]
19. Dragonetti C, Falciola L, Mussini P, Righetto S, Roberto D, Ugo R, Valore A, De Angelis F, Fantacci S, Sgamellotti A, Ramon M, Muccini M. *Inorg. Chem.* 2007; 46:8533. [PubMed: 17883263]
20. Wang B, Liang Y, Dong H, Tan T, Zhan B, Cheng J, Lo KK-W, Lam YW, Cheng SH. *ChemBioChem.* 2012; 13:2729. [PubMed: 23148033]
21. Chen Y, Qiao L, Ji L, Chao H. *Biomaterials.* 2014; 35:2. [PubMed: 24120043]
22. Zhang KY, Liu H-W, Tang M-C, Choi AW-T, Zhu N, Wei X-G, Lau K-C, Lo KK-W. *Inorg. Chem.* 2015; 54:6582. [PubMed: 26087119]
23. Goldstein DC, Peterson JR, Cheng YY, Clady RG, Schmidt TW, Thordarson P. *Molecules.* 2013; 18:8959. [PubMed: 23896620]
24. Shie JJ, Liu YC, Lee YM, Lim C, Fang JM, Wong CH. *J. Am. Chem. Soc.* 2014; 136:9953. [PubMed: 24955871]
25. Barral K, Moorhouse AD, Moses JE. *Org. Lett.* 2007; 9:1809. [PubMed: 17391043]
26. Hong V, Presolski SI, Ma C, Finn MG. *Angew. Chem. Int. Ed.* 2009; 48:9879.
27. Weissleder R. *Nat. Biotechnol.* 2001; 19:316. [PubMed: 11283581]
28. Smith AM, Mancini MC, Nie SM. *Nat. Nanotechnol.* 2009; 4:710. [PubMed: 19898521]
29. Dommerholt J, van Rooijen O, Borrmann A, Guerra CF, Bickelhaupt FM, van Delft FL. *Nat. Commun.* 2014; 5
30. Shieh P, Hangauer MJ, Bertozzi CR. *J. Am. Chem. Soc.* 2012; 134:17428. [PubMed: 23025473]
31. Huang KW, Marti AA. *Anal. Chem.* 2012; 84:8075. [PubMed: 22934684]
32. Staros JV, Bayley H, Standring DN, Knowles JR. *Biochem. Biophys. Res. Commun.* 1978; 80:568.
33. Lo KKW, Chung CK, Lee TKM, Lui LH, Tsang KHK, Zhu NY. *Inorg. Chem.* 2003; 42:6886. [PubMed: 14552640]
34. Edkins RM, Bettington SL, Goeta AE, Beeby A. *Dalton Trans.* 2011; 40:12765. [PubMed: 22002707]
35. Puckett CA, Barton JK. *J. Am. Chem. Soc.* 2007; 129:46. [PubMed: 17199281]
36. Liu XM, Xia H, Gao W, Wu QL, Fan X, Mu Y, Ma CS. *J. Mater. Chem.* 2012; 22:3485.
37. Suntharalingam K, Leczkowska A, Furrer MA, Wu YL, Kuimova MK, Therrien B, White AJP, Vilar R. *Chem. Eur. J.* 2012; 18:16277. [PubMed: 23165895]

**Fig. 1.**

a) Synthesis of compounds. i) NaN<sub>3</sub>; then Ac<sub>2</sub>O.<sup>1</sup> ii) DBU, 83%. iii) [Ir(ppy)<sub>2</sub>(MeCN)<sub>2</sub>][PF<sub>6</sub>], 74%. iv) <sup>t</sup>BuONO and TMS-N<sub>3</sub>, 88% (**5a**), 78% (**5b**), 93% (**5c**). v) phenylacetylene, CuI, 42% (**6a**), 74% (**6b**). (vi) SO<sub>3</sub>·NMe<sub>3</sub>, 44%. b) Emission spectra of **5b** (blue) and **6b** (red). c) Solution of **5a** (left) and **6a** (right) under UV lamp.



**Fig. 2.** Kinetics complex **5d** cycloaddition, assessed by micro plate reader. Emission measured at 600 nm. a) reaction with pentynoic acid in the presence or absence of CuSO<sub>4</sub>, sodium ascorbate, and a triazole ligand THPTA.<sup>26</sup> b) Cu-free reaction with bicyclo[6.1.0]non-4-yne (BCN) derivative **8a** and dibenzocyclooctyne (DBCO) derivative **9**. c) Structure of alkyne used.

**Fig. 3.**

a) Labeling alkyne-tagged BSA with the carboxy complex **5b** in PBS buffer/DMSO (95:5).

b) Analysis of reactions by photoluminescence imaging and total protein stain. c)

Luminescence imaging of a mixture of BSA-Ir (alkyne-tagged BSA reacted with Ir complex **5b**) and MBP-TAMRA (fusion protein of Yes-SH3 and maltose binding protein (MBP) modified with TAMRA-NHS ester).



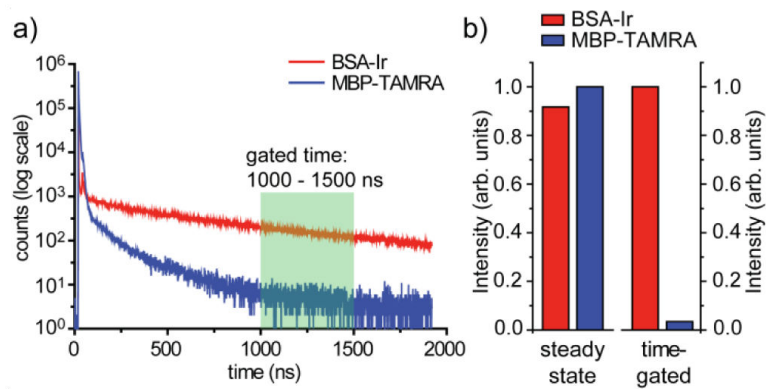


**Fig. 4.**  
a) Photoluminescence time decay for the two bands in Fig. 3c on the PVDF membrane. Excitation with a picosecond 370-nm laser diode and emission collected at 570 nm. b) Comparison of emission intensity using steady-state (left) and time-resolved (1000-1500 ns, right) spectroscopy.

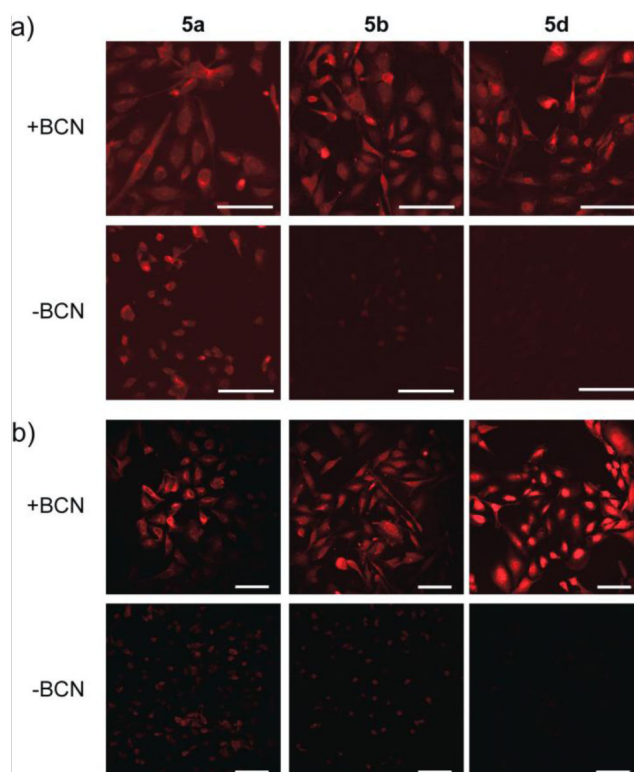


**Fig. 5.** Labeling U2OS cells after treatment with BCN NHS-carbonate **9b**. a) Single-photon excitation luminescence image after treatment with complexes **5a**, **5b**, or **5d**. The emission observed in the absence of BCN varies among three dyes while is comparable in the presence of BCN. b) Two-photon excitation luminescence image of the cells after treatment with azide complexes **5a**, **5b**, and **5d**. (Scale bar: 100  $\mu\text{m}$ ).

**Table 1**

Photoluminescence properties of Ir complexes.

complex	$\lambda_{em}^a$ (nm)	$\epsilon^{a,b}$ ( $M^{-1}cm^{-1}$ )	$\Phi^{a,c}$ (%)	$\tau^{a,d}$ (ns)	brightness <sup>e</sup>	turn-on ratio <sup>f</sup>
amine <b>4a</b>	601	8100	0.13	366	10.5	1.1
azide <b>5a</b>	632	7600	0.13	69	9.5	–
triazole <b>6a</b>	637	8000	1.50	62	119.0	12.5
amine <b>4b</b>	591	9400	0.15	719	14.2	0.80
azide <b>5b</b>	623	9400	0.18	104	17.0	–
triazole <b>6b</b>	590	7200	4.48	104	322.6	19.0
BSA-Ir <sup>g</sup>	571	–	–	1151	–	–

<sup>a</sup> measured in PBS/MeOH (4:1) for **4a-6a** and in PBS/MeOH (95:5) for **4b-6b**.<sup>b</sup> extinction coefficient at 370 nm.<sup>c</sup> quantum yields relative to [Ru(bpy)<sub>3</sub>]Cl<sub>2</sub> reference ( $\Phi = 4.0\%$ ) in air-saturated aq soln.<sup>18</sup><sup>d</sup> photoluminescence lifetime.<sup>e</sup> brightness =  $\epsilon \times \Phi$ .<sup>f</sup> Relative brightness of triazole/azide.<sup>g</sup> carboxylate complex bound to bovine serum albumin on PVDF membrane.